Intracavity coupled-active-resonator-induced dispersion

Yannick Dumeige, Stephane Trebaol, Patrice Feron

Intracavity coupled-active-resonator-induced dispersion

Yannick Dumeige,* Stéphane Trebaol, and Patrice Féron
ENSSAT-FOTON (CNRS-UMR 6082), Université de Rennes 1, 6 rue de Kerampont, Boîte Postale 80518, 22300 Lannion, France
(Received 7 October 2008; published 30 January 2009)

We have proposed and experimentally demonstrated tunable cavity-linewidth narrowing by means of coupled-active-resonator-induced dispersion. We have theoretically studied the coupling-resonator-induced-dispersion phenomenon in the general case of N coupled resonators and especially the case of two or three resonators. In the case of two resonators we have experimentally shown that the strong dispersion induced by the coupling of resonators can lead to cavity ringdown effect enhancement. In the case of three resonators, we propose a coupling scheme allowing the quality (Q) factor of a critically coupled resonator to be increased and actively modulated by using two additional coupled resonators. We have experimentally tested the feasibility of the proposition by using a model system consisting of Er^{3+}-doped fiber coupled resonators. These experimental results demonstrate the possibility of Q-factor tailoring by the use of active artificial photonic media.

DOI: 10.1103/PhysRevA.79.013832 PACS number(s): 42.60.Da, 42.81.Wg, 42.25.Hz

I. INTRODUCTION

High-quality (Q) optical resonators and microresonators [1] are important in a wide range of fields such as nonlinear optics [2,3], cavity ringdown spectroscopy [4], biosensing applications [5], frequency metrology [6] or fundamental physics [7,8]. A lot of studies have been carried out to increase the Q factor of optical cavities by reducing optical losses. Within this framework, resonators with Q factors up to 10^{11} have been demonstrated [9]. Optical losses can also be compensated by using an amplifying medium inside the cavity and thus the Q factor of the resonator can be uniquely limited by the output coupler [10,11]. Generally, the ratio between the coupling coefficient and the optical losses determine the coupling regime of the resonator [12]. Consequently for a given high-Q resonator the output coupler must be adapted in order to achieve optimal or critical coupling [13].

It is also of general interest that the spectral sensitivity of interferometers can be enhanced or actively controlled. The use of slow light or highly dispersive medium [14] can greatly increase the spectral performances of optical interferometers [15,16]. For example, it has been shown that the resolution of Fourier transform interferometers can be enhanced by using atomic vapors as slow-light systems [17]. Optical gyroscope sensibility can be improved by using slow-light media [18,19]. The linewidth of a cavity can also be reduced (and thus the Q factor increased) by introducing a purely dispersive medium inside the cavity [20–22]. The enhancement of the Q factor can even be used to relax the conditions for observing the cavity ringdown effect [23]. In this case the Q factor increase does not rely on the improvement of the optical quality of the medium constituting the resonator, but on the spectral sensitivity of the additional dispersive medium. This has been implemented using coherent effects such as coherent population trapping [20] or electromagnetic-induced transparency (EIT) [24]. The dispersive medium can also be an artificial photonic medium. For example, it has been suggested that using slow Bloch modes would enhance the Q factor of photonic crystal microcavities [25]. Moreover, the use of coupled ring cavities to obtain a composite resonator with a higher finesse than the single ones have also been put forward [26–29]. The first result we would like to present in this paper is that the Q factor increase by means of coupled resonators can lead to the enhancement of the ringdown effect as it has been proposed in coherent media [23].

Microresonators with tunable Q factor are also important for all-optical signal processing based on the dynamic control of the optical properties of photonic structures [30–32]. The Q-factor control has already been suggested and experimentally demonstrated by tuning the coupling properties of two ring resonators by means of thermo-optic [33] or electro-optic effects [32,34]. In this paper we would like also to present our work on the tuning of the Q factor of a ring cavity by coupling it to a system of coupled resonators whose optical losses can be actively modulated. Under particular conditions a transparency window can be induced into the transmission spectrum of two lossy resonators, this phenomenon often referred to as coupled-resonator-induced transparency (CRIT) is a classical counterpart of EIT [35–38]. Moreover, it has been shown that if the losses of the resonators can be controlled by using active resonators, for example, the dispersive properties of this artificial medium can be tailored [39]. Therefore, in this present study we used the CRIT phenomenon using two coupled resonators to control the quality factor of a third ring resonator preserving its coupling properties.

The structure of the paper is as follows. First, we will recall in Sec. II the basic properties of a ring cavity containing a dispersive medium used in the Gires-Tournois interferometer configuration to introduce the main idea and to give a physical insight to our proposition. In this section, we will emphasize the linewidth narrowing due to the spectral sensitivity of the dispersive medium. Section III is devoted to the theoretical description of the Q-factor control by means of dispersion enhancement using coupled resonators. In Sec. III B we will review the phase sensitivity enhancement proposed by Golub in Ref. [28] and study the role of losses. The intracavity coupled-active-resonator-induced dispersion is

*yannick.dumeige@enssat.fr

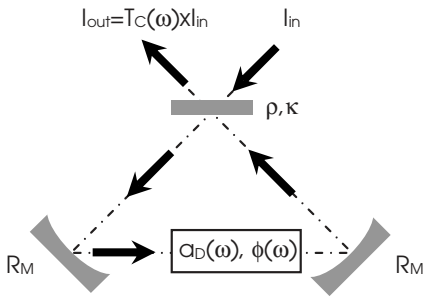

FIG. 1. Sketch of a ring cavity containing a dispersive medium which introduces both phase $\phi(\omega)$ and losses $a_D(\omega)$. The input mirror amplitude reflexion and transmission are ρ and κ. The two other mirrors have perfect reflectivity $R_M=1$. The input I_{in} and output I_{out} intensities are related by the transfer function of the cavity T_C.

presented in Sec. III C. Finally, in Sec. IV we will experimentally demonstrate cavity ringdown effect enhancement and active tuning of resonator Q factor in a fiber optic system.

II. BASIC THEORY

In this section we analyze the effect on the cavity linewidth of an intracavity dispersive medium. First, we will recall the properties of a ring cavity (Fig. 1) consisting of an input coupling mirror with amplitude reflectivity $\rho>0$ and transmittivity $j\kappa$. In this work we only take into account lossless couplers so that $\rho^2+\kappa^2=1$. The two other mirrors perfectly reflect light ($R_M=1$). The static amplitude attenuation of the cavity is noted a_0. The resonator contains a dispersive medium (assumed as punctual) introducing an amplitude (or optical field) attenuation $a_D(\omega)$ and a controllable phase $\phi(\omega)$ depending on the angular frequency $\omega=2\pi\nu$. The total accumulated phase during one round trip in the cavity is $\Phi=\phi+\varphi$ with $\varphi(\omega)=n(\omega)L\omega/c$ where n is the refractive index of the empty cavity (i.e., without the dispersive medium) and L its length. The intensity transmission of the cavity T_C is given in the stationary regime by

$$T_C=\frac{I_{\text{out}}}{I_{\text{in}}}=\frac{\rho^2+a_C^2-2a_C\rho\cos\Phi}{1+a_C^2\rho^2-2a_C\rho\cos\Phi}, \tag{1}$$

where $a_C(\omega)=a_0a_D(\omega)$ is the total amplitude attenuation and I_{in} and I_{out} are defined in Fig. 1. Assuming a weak coupling and low optical losses, the off-resonance value of T_C is maximal and $T_C=T_{\max}\approx 1$. For the resonance frequency $\omega_0=2\pi\nu_0$ such as $\Phi(\omega_0)=0(2\pi)$, the transmission T_C reaches a minimal value,

$$T_{\min}=\frac{[\rho-a_C(\omega_0)]^2}{[1-a_C(\omega_0)\rho]^2}. \tag{2}$$

When $\rho=a_C(\omega_0)$ we have $T_{\min}=0$, the cavity is critically coupled. In this case the extinction ratio defined as $T_{\max}/T_{\min}$ is maximal, and there is a complete transfer of the incident wave optical power to the cavity mode. Still in the high finesse cavity approximation, the linewidth (full width at half-maximum) of $T_C(\omega)$ is given in the phase space by

$$\Delta\Phi_{1/2}=\frac{2[1-a_C(\omega_0)\rho]}{\sqrt{a_C(\omega_0)\rho}}. \tag{3}$$

Assuming a weak variation of phase $d\Phi$ and considering only the first-order term in $d\omega$, we have

$$d\Phi=d\omega\left.\frac{\partial\Phi}{\partial\omega}\right|_{\omega_0}=d\omega\left(\left.\frac{\partial\phi}{\partial\omega}\right|_{\omega_0}+\frac{n_g(\omega_0)L}{c}\right), \tag{4}$$

where n_g is the group index of the empty cavity, thus the angular frequency linewidth $\Delta\omega_{1/2}$ reads as

$$\Delta\omega_{1/2}=\frac{\Delta\Phi_{1/2}}{\tau_G(\omega_0)+\dfrac{n_g(\omega_0)L}{c}}, \tag{5}$$

where $\tau_G=\partial\phi/\partial\omega$ is the group delay introduced by the dispersive medium. Finally, we obtain the expression of the frequency linewidth of the resonator

$$\Delta\nu_{1/2}=\frac{\Delta\nu_{1/2}^0}{1+\dfrac{\tau_G(\omega_0)}{\tau_L(\omega_0)}}, \tag{6}$$

where $\tau_L=n_gL/c$ is the round-trip propagation duration and $\Delta\nu_{1/2}^0$ is the linewidth of the resonator assuming $\varphi(\omega_0)=0(2\pi)$ and no additional dispersion or $\phi(\omega)=0$,

$$\Delta\nu_{1/2}^0=\frac{c[1-a_C(\omega_0)\rho]}{\pi n_g(\omega_0)L\sqrt{a_C(\omega_0)\rho}}. \tag{7}$$

By writing the quality (Q) factor $Q_0=\nu_0/\Delta\nu_{1/2}^0$ of the cavity with no supplementary dispersion, we obtain the expression of the Q factor taking into account the additional dispersion,

$$Q=\frac{\nu_0}{\Delta\nu_{1/2}}=Q_0\left(1+\frac{\tau_G(\omega_0)}{\tau_L(\omega_0)}\right). \tag{8}$$

Equation (8) shows that it is possible to increase the Q factor of a resonator by using a dispersive medium introducing high resonant group delay $\tau_G(\omega_0)$ and no additional optical losses. It is important to note that the introduction of a purely dispersive medium increases the Q factor without changing the coupling properties of the resonator.

III. LINEWIDTH NARROWING BY DISPERSION ENHANCEMENT USING COUPLED RESONATORS

A. Presentation of the generic structure

The generic system we study in this paper consists of N coupled ring resonators as represented in Fig. 2, for $i\in[1,N]$, we call φ_i the round-trip phase accumulated in the loop i of length L_i and a_i the amplitude attenuation introduced by each loop. We assumed that the material constituting the rings is nondispersive ($n_g=n$) thus $\varphi_i(\omega)=n\omega L_i/c$. The resonators are coupled to each other by couplers C_i characterized by coupling coefficients $\rho_i>0$ and $j\kappa_i$ related by $\rho_i^2+\kappa_i^2=1$. We note $t_i(\omega)$ the amplitude transfer function of each stage as represented in Fig. 2. The cavity whose resonance properties will be controlled is loop N and using the

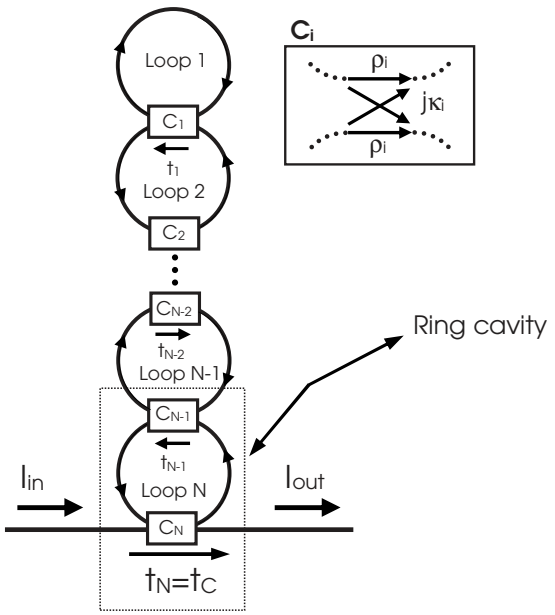

FIG. 2. Cavity linewidth narrowing using $N-1$ ring resonators or optical loops. The dispersive medium is constituted by the coupled ring resonators 1 to $N-1$. The cavity whose Q factor is increased is loop N. The system is coupled to a bus fiber via the coupler C_N. The inset represents coupler C_i for $i \in [1,N]$.

preceding section notations $\rho=\rho_N$, $L=L_N$, $\varphi=\varphi_N$, $a_0=a_N$, $a_D=|t_{N-1}|$, and $\phi=\arg(t_{N-1})$. The cavity transfer function is given by $T_C=|t_C|^2=|t_N|^2$. This last expression is evaluated by the recursive relation for $i \in [1,N]$ [36],

$$t_i = |t_i|e^{j\phi_i} = \frac{\rho_i - t_{i-1}a_i e^{j\varphi_i}}{1 - t_{i-1}\rho_i a_i e^{j\varphi_i}} \tag{9}$$

with the initial value $t_0=1$.

B. Cavity linewidth narrowing using all-pass filters

In this first example the dispersive medium embedded in loop N is constituted by $N-1$ lossless identical loops used as all-pass filters (APF) as suggested in [28], thus $a_i=1$, $\rho_i=\rho$, and $L_i \approx \ell$ for $i \in [1,N-1]$. This purely dispersive medium only introduces a phase shift $\phi_{N-1}=\arg(t_{N-1})$ with $a_{N-1}=|t_{N-1}|=1$ which can be evaluated by calculating recursively the phase shift ϕ_i for $i \in [1,N-1]$,

$$\phi_i = \arg(t_i) = \pi + \varphi_i + \phi_{i-1} + 2\arctan\left(\frac{\rho \sin(\varphi_i + \phi_{i-1})}{1 - \rho\cos(\varphi_i + \phi_{i-1})}\right), \tag{10}$$

with $\phi_0(\omega_0)=0$. We choose $L_1=\ell=M\lambda_0/n$ where $\lambda_0=c/\nu_0$ is the resonant wavelength, $M \in \mathbb{N}$ and $M \gg 1$. With $L_i=L_1+\lambda_0/(2n)$ we have $\varphi_1(\omega_0)=0(2\pi)$ and $\varphi_i(\omega_0)=\pi(2\pi)$ for $i \in [2,N]$. Consequently we obtain $\phi_i(\omega_0)=\pi(2\pi)$ for $i \in [1,N]$ and the resonance condition for $i \in [1,N-1]$,

$$\varphi_i(\omega_0) + \phi_{i-1}(\omega_0) = 0(2\pi), \tag{11}$$

since we have assumed $\rho > 0$. The resonant group delay τ_i defined by,

$$\tau_i = \left.\frac{\partial \phi_i}{\partial \omega}\right|_{\omega_0} \tag{12}$$

can be easily evaluated using the simple recursive relation deduced from Eq. (10),

$$\tau_i = \frac{1+\rho}{1-\rho}(\tau_\ell + \tau_{i-1}), \tag{13}$$

where $\tau_\ell = n\ell/c$ and $\tau_0=0$. Finally we obtain

$$\tau_G(\omega_0) = \tau_{N-1} = \frac{1+\rho}{2\rho}\left[\left(\frac{1+\rho}{1-\rho}\right)^{N-1} - 1\right]\tau_\ell, \tag{14}$$

which can be used in Eq. (8) giving the Q-factor enhancement due to the dispersive medium,

$$Q = Q_0\left\{1 + \frac{1+\rho}{2\rho}\left[\left(\frac{1+\rho}{1-\rho}\right)^{N-1} - 1\right]\frac{\ell}{L}\right\}. \tag{15}$$

Assuming that $L \approx \ell$ we have

$$Q = Q_0\frac{1+\rho}{2\rho}\left[\left(\frac{1+\rho}{1-\rho}\right)^{N-1} + \frac{\rho-1}{\rho+1}\right], \tag{16}$$

which can be written in the high finesse cavity approximation ($\rho \approx 1$),

$$Q \approx Q_0\left(\frac{2}{1-\rho}\right)^{N-1} \tag{17}$$

which can also be written using the linewidth of the resonator

$$\Delta\nu_{1/2} \approx \Delta\nu_{1/2}^0\left(\frac{1-\rho}{2}\right)^{N-1}. \tag{18}$$

These results, consistent with those presented in [26,28], show that the cavity linewidth can be drastically reduced assuming all the additional resonators are lossless. We illustrate this phenomenon by calculating the intensity transfer function $T_C=|t_2|^2$ in the simplest case of two identical coupled resonators with $\rho=\rho_1=\rho_2=0.95$. Since the cavity is critically coupled ($a_2=0.95$), the finesse of the cavity (loop 2) is $F=1/(\Delta\nu_{1/2}^0\tau_L)=\pi\rho_2/(1-\rho_2^2)\approx 30.6$.

The results are shown in Fig. 3 representing T_C as a function of the normalized detuning $\delta/\Delta\nu_{1/2}^0$ with $\delta=\nu-\nu_0$. This spectrum shows simultaneously the resonances of the empty cavity for $\delta/\Delta\nu_{1/2}^0=\pm F/2$ whose linewidths are $\Delta\nu_{1/2}^0$ and the composite enhanced resonance for $\delta=0$ whose Q factor is increased by a factor $2/(1-\rho)=40$ with respect to the two other resonances. Note that since we have chosen $a_1=1$ the three resonances are critically coupled.

If now we consider the same optical losses in each resonator, $a_i=a<1$, the resonant amplitude transmission can be simply written for $i \in [2,N-1]$,

$$t_i(\omega_0) = \frac{at_{i-1}(\omega_0) + \rho}{\rho a t_{i-1}(\omega_0) + 1} \tag{19}$$

with $t_1(\omega_0)=(\rho-a)/(1-\rho a)<0$. The general term of this homographic recursive sequence can be calculated as

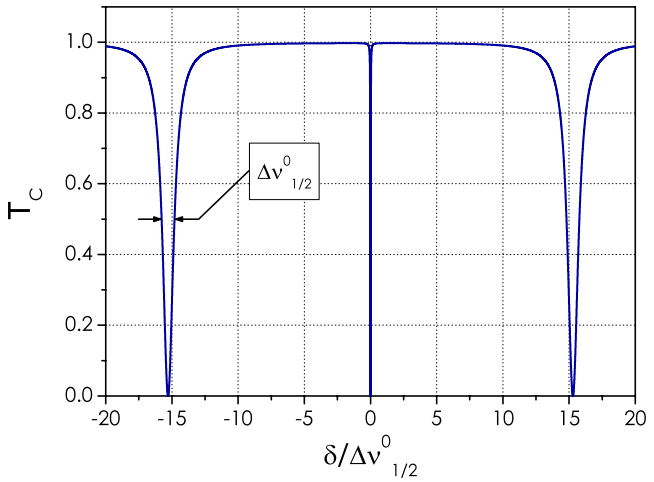

FIG. 3. (Color online) Transmission spectrum $T_C=|t_2|^2$ in the case of $N=2$ nearly identical resonators $L_2=L_1+\lambda_0/(2n)$ with $a_2=\rho=\rho_1=\rho_2=0.95$ and $a_1=1$.

$$t_i(\omega_0)=\frac{\Lambda^- - y_1\Lambda^+ k^{i-1}}{1-y_1 k^{i-1}}, \tag{20}$$

where we note

$$\Lambda^{\pm}=\frac{a-1\pm\sqrt{(1-a)^2+4a\rho^2}}{2a\rho} \tag{21}$$

and define

$$k=\frac{a+1+\sqrt{(1-a)^2+4a\rho^2}}{a+1-\sqrt{(1-a)^2+4a\rho^2}}>1 \tag{22}$$

with $y_1=[t_1(\omega_0)-\Lambda^-]/[t_1(\omega_0)-\Lambda^+]$. Since $k>1$ the resonant amplitude transmission $t_i(\omega_0)$ tends to $\Lambda^+>0$, thus from a particular value $i_{\max}$ of i the resonant transmission $t_{i_{\max}}(\omega_0)$ becomes positive.

In this case, the resonance condition given by Eq. (11) is no longer fulfilled and the loop N becomes off resonance. Consequently the additional dispersive medium only introduces losses and its beneficial impact on the Q factor is canceled. For low losses ($a\approx 1$), keeping only the first-order terms in $1-a$ we obtain

$$\Lambda^{\pm}\approx\frac{(a-1)(1\mp\rho)}{2\rho}\pm 1 \tag{23}$$

and $k\approx(1+\rho)/(1-\rho)$. y_1 can also be approximately calculated by

$$y_1\approx-\frac{(1-a)(1+\rho)^2}{4\rho(1-\rho)}. \tag{24}$$

Thus the effective resonator number $i_{\max}$ is calculated using Eq. (20) by $i_{\max}=1+\mathrm{E}[f(a,\rho)]$ where we define

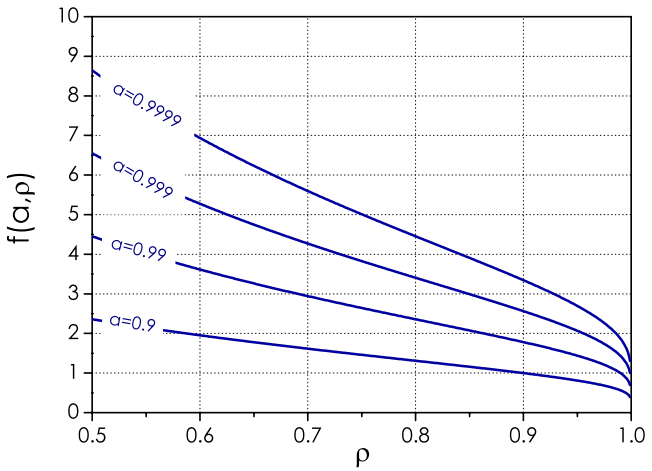

FIG. 4. (Color online) Function $f(a,\rho)$ giving the effective number of resonators by $i_{\max}=1+\mathrm{E}[f(a,\rho)]$ as a function of ρ for different values of round-trip amplitude attenuation a.

$$f(a,\rho)=1+\frac{\ln\left(\frac{\Lambda^-}{y_1\Lambda^+}\right)}{\ln k} \tag{25}$$

and $\mathrm{E}[x]$ as the whole part of x. Using the previous first-order approximations in $1-a$ we finally obtain

$$f(a,\rho)\approx 1+\frac{\ln[4\rho(1-\rho)]-\ln[(1+\rho)^2(1-a)]}{\ln(1+\rho)-\ln(1-\rho)}. \tag{26}$$

Figure 4 represents $f(a,\rho)$ and thus $i_{\max}$ as a function of ρ for different values of a. First, for a fixed amplitude attenuation the number of useful resonators decreases when the coupling coefficient ($\kappa=\sqrt{1-\rho^2}$) between resonators decreases. Second, for a given value of ρ or coupling coefficient between resonators, optical losses limits the number of useful resonators. This limitation increases when ρ decreases. Finally, these results show that even with a very low attenuation the resonator number $(N-1)$ is severely limited. Moreover, for low values of $N-1$, the optical losses must be rigorously controlled in the first resonators where their detrimental role is enhanced.

To illustrate this last property we have calculated the cavity transmission $T_C=|t_3|^2$ for $N=3$ with $L_3=L_2=L_1+\lambda_0/(2n)$, $a_3=\rho_1=\rho_2=\rho_3=0.95$. The results are given in Fig. 5 which represents the transmission T_C as a function of the normalized detuning $2\delta/\Delta\nu^0_{1/2}$. For $a_1=a_2=1$ the cavity remains critically coupled and the linewidth is reduced by a factor of about 1600 given by Eq. (18). If we add low losses into the first resonator ($a_1=0.9995$ and $a_2=1$), the resonance is much more broadened than in the case where we add the same losses into the second resonator ($a_1=1$ and $a_2=0.9995$). Moreover, in this configuration the resonance transmission value $T_C(0)$ depends strongly on the loss values in the additional resonators which modifies the coupling properties of the cavity. In our example with losses in resonators 1 or 2 the cavity is no longer critically coupled.

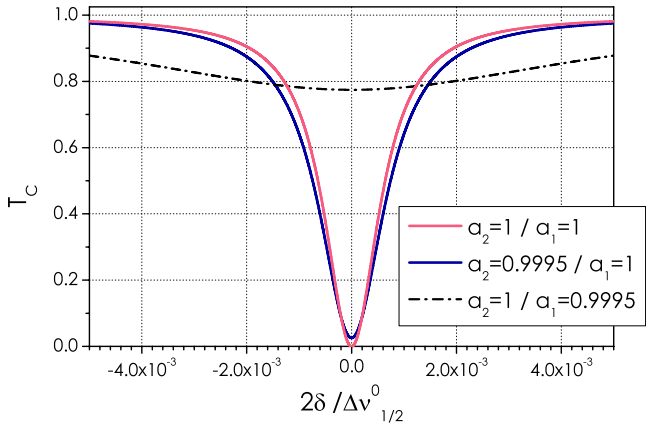

FIG. 5. (Color online) Transmission spectrum $T_C=|t_3|^2$ in the case of $N=3$ nearly identical resonators $L_3=L_2=L_1+\lambda_0/(2n)$ with $a_3=\rho_1=\rho_2=\rho_3=0.95$ for different values of losses in resonators 1 and 2.

C. Intracavity coupled-active-resonator-induced dispersion

In this second example we propose to use CRIT which is the classical counterpart of coherent effects such as EIT. In this section, we will show that using this resonator coupling scheme, it is possible, as demonstrated in atomic systems, to actively control the quality factor of the ring resonator by preserving its coupling properties [20]. The system of interest consists of two coupled resonators (loops 1 and 2) which mimic the dispersive medium introducing $\phi(\omega)$. The third resonator (loop 3) is the cavity whose quality factor Q is controlled as it was the case in the preceding section (see Fig. 6). Referring to Sec. II the amplitude and the phase of the dispersive medium are $a_D=|t_2|$ and $\phi=\phi_2=\arg(t_2)$, the cavity is loop 3: $\rho=\rho_3$ and $L=L_3$ and the cavity transfer function is given by $T_C=|t_C|^2=|t_3|^2$. In this section we want

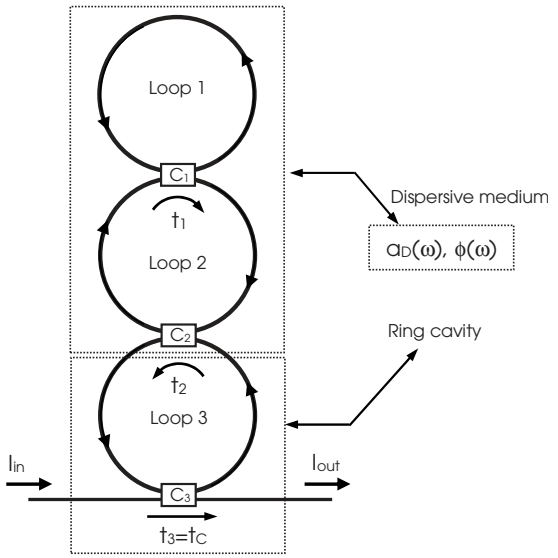

FIG. 6. Schematic representation of the proposition of intracavity coupled-resonator-induced dispersion using fiber loops. The dispersive medium is constituted by the two coupled ring resonators 1 and 2. Here we increase the loop 3 Q factor.

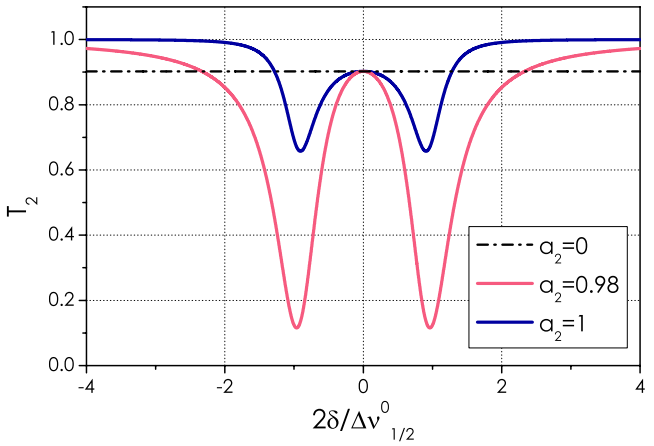

FIG. 7. (Color online) Intensity transmission spectrum $T_2=|t_2|^2$ of the dispersive medium for three values of a_2.

to show the unique effect of the additional dispersive medium. Thus we will compare the two following situations: (i) $a_2=0$ allowing a decoupling of loop 3 which corresponds to the case of an empty cavity (only loop 3), (ii) the case where $a_2\neq 0$, where the cavity is connected to the dispersive medium. As already underlined, the two previous cases must correspond to a critically coupled cavity (loop 3) to be comparable. Consequently we must have $|t_2(\omega_0,a_2=0)|=|t_2(\omega_0,a_2\neq 0)|=a_D(\omega_0)$ and $a_C(\omega_0)=a_D(\omega_0)a_3=\rho_3$. Assuming $\rho_1=a_1$ and $\varphi_1(\omega_0)=\varphi_2(\omega_0)=0(2\pi)$, using Eq. (9) we note that $t_2(\omega_0)=\rho_2$ for any value of a_2. It is crucial to note that $t_2(\omega_0)$ is real which implies that $\phi(\omega_0)=\phi_2(\omega_0)=0(2\pi)$, and thus the resonance frequency of the cavity (loop 3) remains unaffected by the presence of the dispersive medium (loops 1 and 2). If we consider that all the loops have the same length $L_1=L_2=L$ and thus the same resonant angular frequency ω_0 since $\varphi(\omega_0)=\varphi_1(\omega_0)=\varphi_2(\omega_0)=0(2\pi)$, the resonant group delay is given by

$$\tau_G(\omega_0)=a_2\frac{\rho_1(1-\rho_2^2)}{\rho_2(1-\rho_1^2)}\tau_L, \tag{27}$$

in that case the linewidth of the cavity is

$$\Delta\nu_{1/2}=\frac{\Delta\nu_{1/2}^0}{1+a_2\dfrac{\rho_1(1-\rho_2^2)}{\rho_2(1-\rho_1^2)}}. \tag{28}$$

By choosing, for example, $a_3=1$ and $\rho_2=\rho_3$, we obtain a critically coupled cavity in the two cases (i) and (ii). We illustrate our approach using three loops of equal length and refractive index with $\rho_1=a_1=0.995$ and $\rho_2=\rho_3=0.95$. We recall that the three resonators have the same resonance frequency ν_0. Figure 7 represents the intensity transfer function of the artificial dispersive medium $T_2=|t_2|^2$ for different values of a_2. The transmission resonance is split and the resonant value of transmission is $T_2(\delta=0)=\rho_2^2\approx 0.9$ whatever the value of a_2. We also represent the phase shift $\phi_2(\delta)$ and the group delay $\tau_G=\partial\phi_2/\partial\omega$ introduced by the dispersive medium (Fig. 8). For $a_2=0$ the dispersive medium only introduces losses whereas for $a_2\neq 0$, in the represented frequency

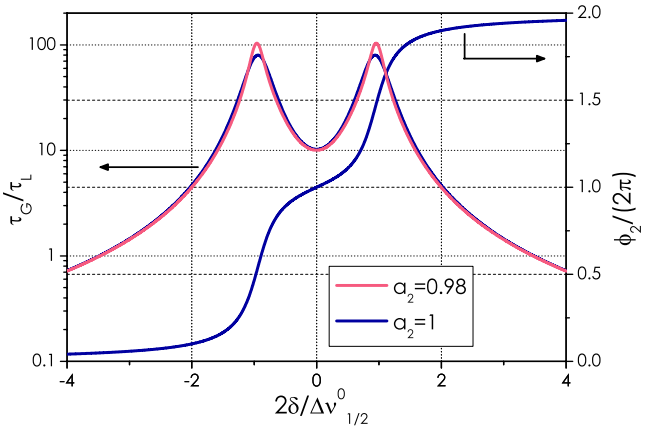

FIG. 8. (Color online) Phase shift $\phi=\phi_2$ (right axis) and group delay dispersion $\tau_G=\partial\phi_2/\partial\omega$ (left-hand axis) of the artificial dispersive medium. We represent the phase shift only for $a_2=1$.

range, all the frequency components are delayed. At resonance ($\delta=0$) for $a_2=1$ the delay is approximately $\tau_G(\delta=0) \approx 10.2\tau_L$ thus we expect a narrowing of the linewidth of about one order of magnitude. This is verified by calculating the transfer function of the cavity $T_C=|t_3|^2$ for different values of a_2 ranging from $a_2=0$ to $a_2=1$ as represented in Fig. 9. First, it can be noted that from $a_2=0$ to $a_2=1$, the resonance width of the cavity is strongly reduced and the cavity remains critically coupled.

In Fig. 10 we have represented simultaneously the case $a_2=0$ and $a_2=1$. In this example, we show that by only controlling the losses in loop 2 (a_2), it is possible to reduce the linewidth of the resonator by a factor 11.2, in good agreement with the first-order calculation of Eq. (7). The two additional transmission dips of Fig. 11 representing the two cases $a_2=0.98$ and $a_2=0$ come from the splitting of the common resonance ν_0 of the three resonators.

IV. EXPERIMENTAL RESULTS

In this section cavity linewidth narrowing using coupled resonators is verified in a simple model system consisting of

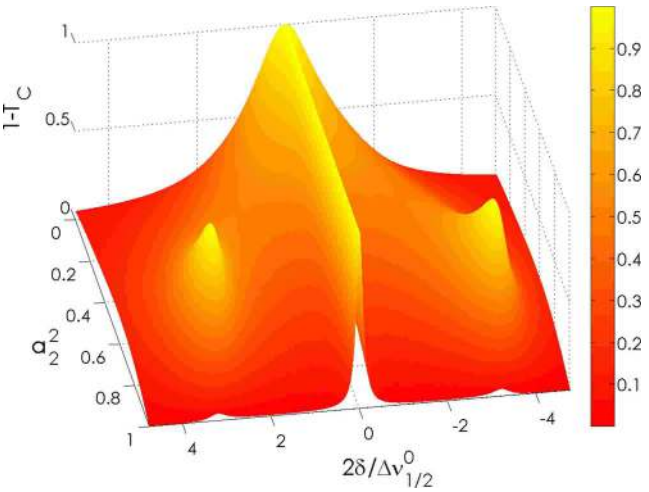

FIG. 9. (Color online) Cavity absorption $1-T_C(\delta)$ for intensity attenuation a_2^2 in loop 2 ranging from 0 to 1.

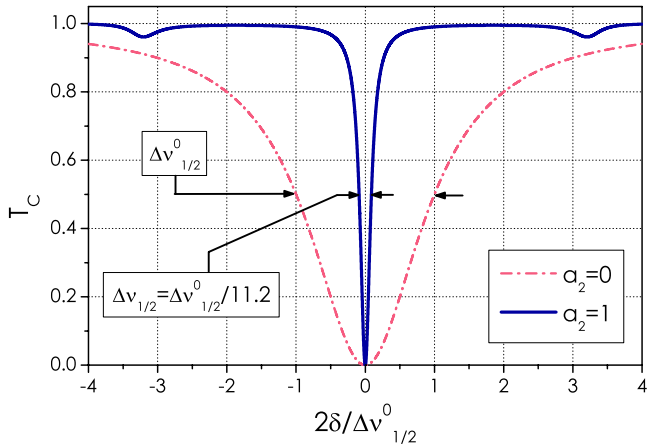

FIG. 10. (Color online) Transmission of the cavity $T_C=|t_3|^2$ for $a_2=0$ and $a_2=1$ (the data are extracted from Fig. 9). We observe a narrowing of the transmission dip by a factor 11.2. In both cases, the cavity remains critically coupled.

Er^{3+}-doped optical fiber loops. We show in Sec. IV B that the cavity ringdown effect can be enhanced using one coupled resonator in the all-pass filter configuration. This effect can be seen as the classical counterpart of the cavity ringdown effect enhancement based on EIT as proposed in Ref. [23]. In Sec. IV C, we demonstrate intracavity coupled-active-resonator-induced dispersion and we show that it is possible to actively tune the Q factor of a resonator by using artificial coupled resonator dispersion.

A. Experimental setup and methods

The experimental setup consisting of N standard optical fiber loops is described in Fig. 12. For the experimental test of Q-factor enhancement using an APF, we used only $N=2$

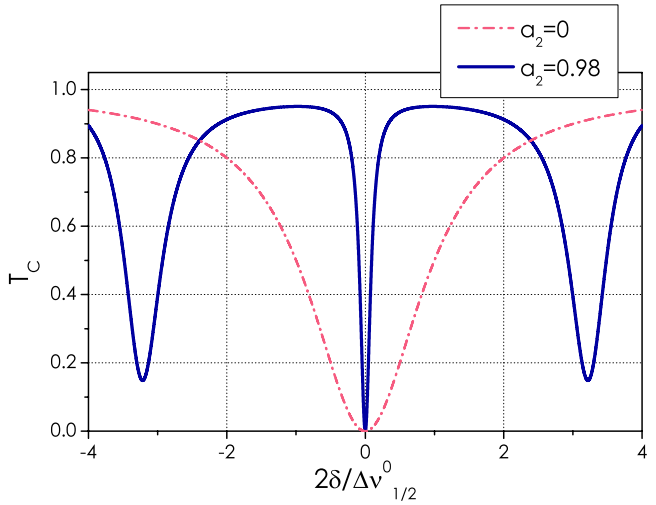

FIG. 11. (Color online) Transmission of the cavity $T_C=|t_3|^2$ for $a_2=0$ and $a_2=0.98$ (the data are extracted from Fig. 9). We observe the same narrowing of the transmission dip as in Fig. 10. The dips coming from the coupling of the three resonators are stronger than in the previous case.

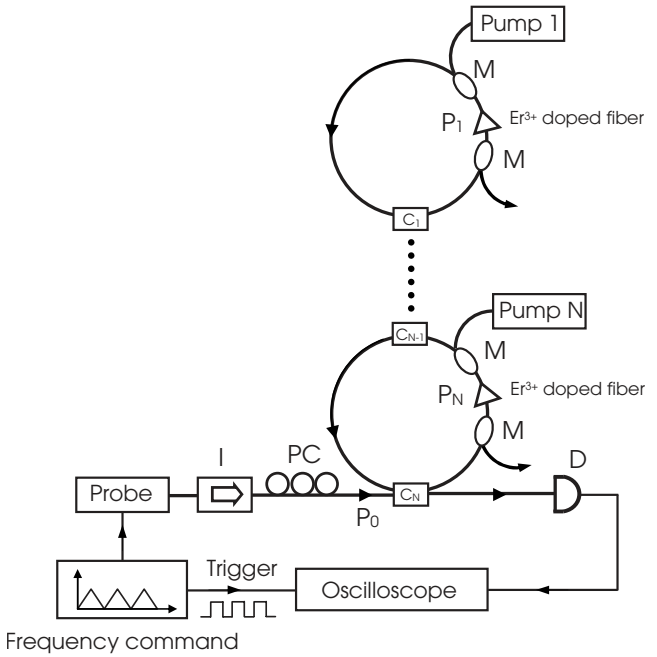

FIG. 12. The experimental setup is composed of N active Er^{3+}-doped fiber loops coupled to a bus fiber. PC is a polarization controller and I an optical isolator. M are wavelength division multiplexers allowing the insertion of the 980 nm pump lasers i where $i \in [1,N]$. P_i are the injected pump powers. $P_0=1$ mW is the optical power entering the cavity. D is an optical detector. The probe is a tunable 1550 nm laser diode (linewidth 150 kHz) whose central frequency is linearly swept with a controllable period. To limit thermal fluctuations, we immersed the coupled rings in a water bath.

loops whereas the intracavity coupled-resonator-induced-dispersion effect requires $N=3$ loops.

Since all the effects presented in the previous theoretical sections rely on very low loss resonator or optical loss modulation, we used Er^{3+}-doped fibers which allow us to compensate for or to introduce optical losses by varying independently the pumping rates of 980 nm laser diodes as shown in Fig. 12. To probe the coupled resonators we used an external cavity laser tunable around $\lambda_0=1550$ nm. The central frequency of the probe laser is linearly swept and the transmission of the system is simultaneously recorded. Assuming a slow scanning of the probe frequency, the stationary response of the resonators can be deduced from the temporal recording using a calibration of the frequency sweeping speed [10,40]. If the probe wavelength is swept faster than the cavity lifetime, the output intensity shows oscillations. This phenomenon is known as the cavity ringdown effect and has several interesting applications in cavity ringdown spectroscopy, for example, [23,41–43]. For high quality resonators this effect must be taken into account in order to determine precisely their finesse [7,44] and can be used to determine unambiguously their coupling regime [45]. Note that the apparition of the cavity ringdown effect for a low sweeping speed is the manifestation of a very narrow resonance [23]. The output temporal profile for a single resonator (without additional dispersive medium) has been derived in several works [42,44,45], and we give here only the relevant results which are indispensable to characterize our resonators.

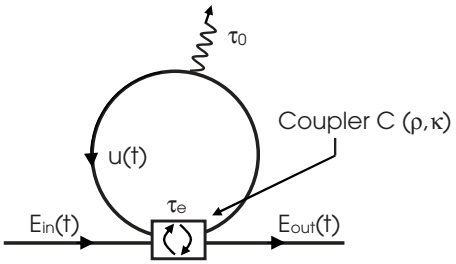

FIG. 13. Schematic description of the parameters used in the calculation of the temporal evolution of the resonator mode amplitude $u(t)$. τ_0 is the intrinsic cavity lifetime associated with optical losses and τ_e is the external cavity lifetime associated with coupler C.

We consider here a single mode resonator whose amplitude round attenuation is a_0, the coupling coefficient are (ρ,κ) and the resonant frequency is ω_0 as represented in Fig. 13. If we call u the resonator mode amplitude [46], its time evolution can be deduced from

$$\frac{du}{dt} = \left(j\omega_0 - \frac{1}{\tau}\right)u(t) + \sqrt{\frac{2}{\tau_e}}E_{\text{in}}(t). \tag{29}$$

$\tau=2Q/\omega_0$ is the amplitude cavity lifetime, it is related to the amplitude intrinsic cavity lifetime $\tau_0=\tau_L(\omega_0)\sqrt{a_0}/(1-a_0)$ and to the external cavity lifetime $\tau_e=\tau_L(\omega_0)\sqrt{\rho}/(1-\rho)$ by $1/\tau=1/\tau_0+1/\tau_e$. In our experiment we use a frequency swept input field which can be written $E_{\text{in}}(t)=E_0e^{j\omega(t)\cdot t}$ where $\omega(t)=\omega_i+V_St/2$ (note that V_S represents the angular frequency sweeping speed). In this case Eq. (29) can be analytically integrated and the mode amplitude is thus given by

$$u(t) = \sqrt{\frac{2}{\tau_e}}E_0\exp\left(j\omega_0 t - \frac{t}{\tau}\right)\left(f(t) - f(0) + \frac{1}{j(\omega_i-\omega_0)+1/\tau}\right) \tag{30}$$

which can be expressed using the complex error function $\text{erf}(z)$ with $z \in \mathbb{C}$,

$$f(t) = -\sqrt{\frac{j\pi}{2V_S}}\exp\left(\frac{-j(2\pi\delta_i - j/\tau)^2}{2V_S}\right)\text{erf}\left(\frac{j/\tau - 2\pi\delta_i - V_St}{\sqrt{2jV_S}}\right), \tag{31}$$

where $2\pi\delta_i=\omega_i-\omega_0$ is the initial detuning. The output field can be calculated by

$$E_{\text{out}}(t) = -E_{\text{in}}(t) + \sqrt{\frac{2}{\tau_e}}u(t), \tag{32}$$

which allows the intensity transmission to be deduced using $T_C=|E_{\text{out}}|^2/E_0^2$. From an experimental point of view, we record the experimental temporal variations of the transmission T_{mes}, which are compared to the theoretical value T_{theo} by using the least square method,

$$\sigma^2(\tau_0,\tau_e,V_S) = \sum_{i=1}^{q}[T_{\text{mes},i} - T_{\text{theo},i}(\tau_0,\tau_e,V_S)]^2, \tag{33}$$

where q is the number of temporal sampling points. The value of σ^2 is minimized by automatically changing the value of τ_0, τ_e, and V_S to obtain the best fit. It is possible to infer a measurement of all the characteristics of the resonator from the values of the two cavity lifetimes τ_0 and τ_e.

B. Cavity ringdown effect enhancement using coupled resonators

First, we test the possibility to increase the quality factor of a resonator by introducing inside the cavity an APF as shown in Sec. III B. We use two fiber rings, loop 2 is the cavity whose Q factor will be increased and loop 1 plays the role of the APF. The length of the two resonators are almost equal, $L_1=2.01$ m and $L_2=2.00$ m. In loop 2 the Er^{3+} section is 30 cm long whereas in loops 1 the Er^{3+} section is 1 m long. The effective refractive index of the optical fibers is $n=1.46$. The nominal power coupling ratios are $\rho^2=\rho_1^2=\rho_2^2=90\%$ and $\kappa_1^2=\kappa_2^2=10\%$ for both couplers C_1 and C_2. The pumping rate $P_2=5.3$ mW is optimized to obtain a critical coupling for all the resonances, whereas we used a high pumping rate $P_1=22.8$ mW to compensate for the optical losses in loop 2. We use a slow scanning rate, $V_S/(2\pi)\approx 0.4$ MHz/μs (note that this calibration is made using the free spectral range of loop 2). The corresponding spectrum is given in Fig. 14(a). We obtain two resonances associated with the empty cavity for $\delta=0$ and $\delta=103$ MHz. The theoretical curve is obtained considering an empty cavity and using the nominal values already given ($a_2=\rho_2=\sqrt{0.9}\approx 0.95$, $L_2=2.00$ m, and $n=1.46$). From this fit we obtain $\Delta\nu_{1/2}^0\approx 3.4$ MHz and thus $Q_0=5.7\times 10^7$. Between these two resonances we can distinguish the very narrow composite resonance. This experimental spectrum is useful since it shows both the empty cavity resonances and the enhanced resonances due to loop 1. Even though the sweeping rate is low, since the coupling with loop 1 greatly increases the Q factor of loop 2 we observe oscillations due to the cavity ringdown effect. Figure 14(b) represents the cavity ringdown oscillations due to the narrow enhanced resonance as a function of time.

By using the procedure described in Sec. IV A and Eq. (33) we obtain the theoretical fit also given in Fig. 14(b) from which we infer $\tau_0=2.48$ μs and $\tau_e=14.3$ μs. These values give $\tau=2.11$ μs and thus $Q=1.3\times 10^9$ corresponding to an experimental Q-factor enhancement of about $Q/Q_0\approx 23$. For a resonator including a dispersive medium, the relation between the attenuation and the intrinsic cavity lifetime must be changed as follows taking into account the group delay of the whole system:

$$\tau_0=\frac{[\tau_L(\omega_0)+\tau_G(\omega_0)]\sqrt{a_0a_D(\omega_0)}}{1-a_0a_D(\omega_0)}, \tag{34}$$

we make the same change in the relation between the coupling coefficient and the external cavity lifetime,

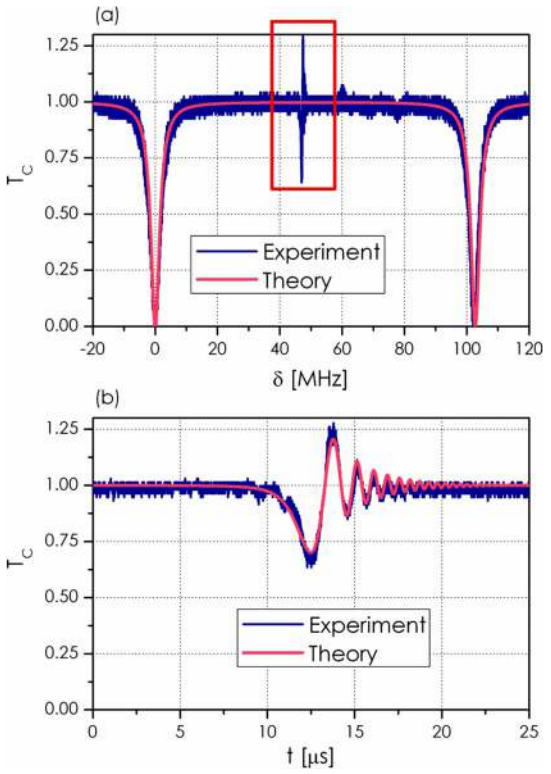

FIG. 14. (Color online) (a) Experimental spectrum of the transmission of the cavity (loop 2) in the case $N=2$. We also give the theoretical calculation corresponding to the nominal values of the experimental parameters assuming loop 2 alone. (b) Time profile of the cavity ringdown oscillations corresponding to the box of (a). We also give the theoretical calculations.

$$\tau_e=\frac{[\tau_L(\omega_0)+\tau_G(\omega_0)]\sqrt{\rho}}{1-\rho}. \tag{35}$$

In the present case, $\rho=\rho_2=0.95$ and $\tau_L=nL_2/c\approx 9.7$ ns, using Eq. (35) we obtain $\tau_G(\omega_0)\approx 724$ ns. Assuming $a_1\approx 1$, we have $\tau_G(\omega_0)=\tau_L(1+\rho_1)/(1-\rho_1)$ (since $L=L_2\approx L_1$), thus we can calculate $\rho_1\approx 0.9735$. Using Eq. (34) and considering $a_0=a_2\approx 0.95$ we obtain the value of $a_D(\omega_0)=|t_1|\approx 0.7832$. Finally, the value of the amplitude attenuation in loop 1 $a_1=0.9967$ is deduced from $|t_1|=(a_1-\rho_1)/(1-\rho_1a_1)$. The experimental values of a_1 and ρ_1 show that the pumping of loop 1 is nearly optimal and that the inferred coupling value is in agreement with the nominal value ($0.97^2\approx 94\%$ keeping only two digits).

C. Intracavity coupled-active-resonator-induced dispersion

To experimentally test the intracavity coupled-resonator-induced-dispersion effect, we connect a third shorter fiber

TABLE I. Description of the resonators used in the experimental demonstration of intracavity active-resonator-induced dispersion.

Loop 1	$L_1=1.41$ m	Coupler C_1	$\rho_1^2=99\%$	$\kappa_1^2=1\%$
Loop 2	$L_2=2.01$ m	Coupler C_2	$\rho_2^2=90\%$	$\kappa_2^2=10\%$
Loop 3	$L_3=2.00$ m	Coupler C_3	$\rho_3^2=90\%$	$\kappa_3^2=10\%$

loop to the system. The length of the ring resonators and their associated nominal power coupling ratios are given in Table I. In loops 1 and 3 the Er^{3+} section is 30 cm long whereas in loops 2 the Er^{3+} section is 1 m long. We use a longer doped fiber section in loop 2 since we want to reach both high absorption ($a_2 \approx 0$) and low losses ($a_2 \approx 1$) in the same fiber. Without pumping of loop 2 the Er^{3+}-doped section induced absorption of about 11.2 dB. Since the core diameter of the doped fiber is about only 4 μm, the loss splicing are high which allows a low value of a_2 to be obtained.

As already mentioned, since the values of a_1 and a_3 depend on coupling values of C_1 and C_3 we also used Er^{3+}-doped fiber in loops 1 (with $P_1=18.6$ mW) and 3 (with $P_3=8.3$ mW) in order to try to obtain the condition described in the preceding section. Figure 15 represents the transfer function $T_C=T_3$ without pumping (a) $P_2=0$ and with pumping (b) $P_2=40.2$ mW of loop 2. Even though the resonance frequency of loops 3 remains theoretically unchanged by the pumping of loop 2, experimentally the two spectra of Fig. 15 were not aligned due to thermal drifts. We also give theoretical calculations associated with these experimental results. We used the following procedure to obtain the theoretical fit: We fixed ρ_1 to its nominal value ($\rho_1=0.995$), ρ_2 and ρ_3 are fixed to the values found in the previous experiment ($\rho_2=0.97$ and $\rho_3=0.95$). We set the lengths to their measured values and the refractive index is still $n=1.46$. To fit the transmission spectrum of Fig. 15(a) without pumping of loop 2 we also fixed $a_2=0$ and we adjust the value of losses in loop 3 to $a_3=0.95$. To fit the transmission spectrum of Fig. 15(b) we keep the previous value of a_3 and we adjust $a_2=0.97$ and $a_1=0.985$. We infer a linewidth of $\Delta\nu_{1/2}^0=4.3$ MHz from the theoretical fit without pumping and we measure a reduction of the linewidth to $\Delta\nu_{1/2}=790$ kHz when loop 2 is pumped. We obtain a good agreement between the experiment and the calculations. The parameter values inferred from the fit show that the losses are not totally compensated in loops 1 and 2 whereas in the case of $N=2$ (see Sec. IV B) the losses in loop 1 were almost compensated. This difference comes from the fact that in the whole transmission spectrum the spectral range where the double resonance condition is verified is wider than the spectral range where the triple resonance is met due to the vernier effect. Consequently it is easier to find an experimental situation where the case $N=2$ is almost optimal as presented in Sec. IV B than to obtain the ideal case corresponding to intracavity coupled-resonator-induced dispersion with $N=3$.

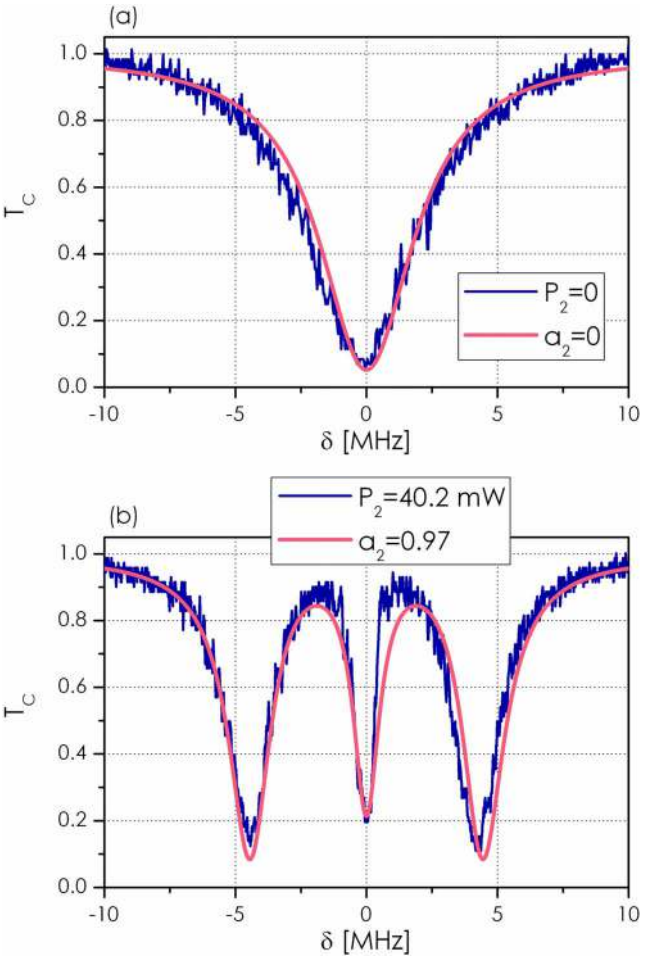

FIG. 15. (Color online) Experimental spectrum of the transmission of the cavity (loop 3): (a) Without pumping of loop 2 and (b) with pumping of loop 2. We also give the theoretical fit obtained using (a) $a_1=0.985$, $\rho_1=0.995$, $a_2=0$, $\rho_2=0.97$, and $a_2=\rho_2=0.95$; (b) $a_1=0.985$, $\rho_1=0.995$, $a_2=0.97$, $\rho_2=0.97$, and $a_2=\rho_2=0.95$.

V. CONCLUSION

The optical cavity Q-factor enhancement by means of intracavity coupled-resonator-induced dispersion have been studied. We have theoretically analyzed the general case of N resonators. We have highlighted the crucial role of optical losses. In the case of $N=3$ resonators we have also suggested to use active resonators with controllable high artificial dispersion to tune the Q factor of a ring resonator without changing its coupling properties and its resonance frequency. We have experimentally tested these two approaches using a model system consisting of Er^{3+}-doped fibers. We have shown that the use of coupled resonators can enhance the cavity ringdown effect. We have also shown that it is possible to change the Q factor of a given resonance without changing its coupling characteristics by modulating the optical losses. This last phenomenon could be of interest in the case of planar active semiconductor coupled microresonators [47,48] for the integration of all-optical signal processing functions.

ACKNOWLEDGMENTS

This work was supported by French "Agence Nationale de la Recherche" through the project O^2E (NT05-3-45032) and by the Centre National d'Études Spatiales (convention No. 60281/00). We wish to thank S. Bodros for helpful discussions.

[1] K. Vahala, *Optical Microcavities* (World Scientific, Singapore, 2004).
[2] T. J. Kippenberg, S. M. Spillane, and K. J. Vahala, Phys. Rev. Lett. **93**, 083904 (2004).
[3] V. S. Ilchenko, A. A. Savchenkov, A. B. Matsko, and L. Maleki, Phys. Rev. Lett. **92**, 043903 (2004).
[4] G. Berden, R. Peeters, and G. Meijer, Int. Rev. Phys. Chem. **19**, 565 (2000).
[5] S. Arnold, M. Khoshsima, I. Teraoka, S. Holler, and F. Vollmer, Opt. Lett. **28**, 272 (2003).
[6] P. Del'Haye, A. Schliesser, O. Arcizet, T. Wilken, R. Holzwarth, and T. J. Kippenberg, Nature (London) **450**, 1214 (2008).
[7] L. Matone, M. Barsuglia, F. Bondu, F. Cavalier, H. Heitmann, and N. Man, Phys. Lett. A **271**, 314 (2000).
[8] T. Aoki, B. Dayan, E. Wilcut, W. P. Bowen, A. S. Parkins, T. J. Kippenberg, K. J. Vahala, and H. J. Kimble, Nature (London) **443**, 671 (2006).
[9] A. A. Savchenkov, A. B. Matsko, V. S. Ilchenko, and L. Maleki, Opt. Express **15**, 6768 (2007).
[10] J. M. Choi, R. K. Lee, and A. Yariv, Opt. Lett. **26**, 1236 (2001).
[11] K. Totsuka and M. Tomita, Opt. Lett. **32**, 3197 (2007).
[12] A. Yariv, Electron. Lett. **36**, 321 (2001).
[13] M. C. Cai, O. Painter, and K. J. Vahala, Phys. Rev. Lett. **85**, 74 (2000).
[14] L. V. Hau, S. E. Harris, Z. Dutton, and C. H. Behroozi, Nature (London) **397**, 594 (1999).
[15] M. Xiao, Y.-Q. Li, S.-Z. Jin, and J. Gea-Banacloche, Phys. Rev. Lett. **74**, 666 (1995).
[16] G. T. Purves, C. S. Adams, and I. G. Hughes, Phys. Rev. A **74**, 023805 (2006).
[17] Z. Shi, R. W. Boyd, R. M. Camacho, Praveen Kumar Vudya Setu, and J. C. Howell, Phys. Rev. Lett. **99**, 240801 (2007).
[18] J. Scheuer and A. Yariv, Phys. Rev. Lett. **96**, 053901 (2006).
[19] M. S. Shahriar, G. S. Pati, R. Tripathi, V. Gopal, M. Messall, and K. Salit, Phys. Rev. A **75**, 053807 (2007).
[20] G. Müller, M. Müller, A. Wicht, R.-H. Rinkleff, and K. Danzmann, Phys. Rev. A **56**, 2385 (1997).
[21] M. D. Lukin, M. Fleischhauer, M. O. Scully, and V. L. Velichansky, Opt. Lett. **23**, 295 (1998).
[22] M. Soljačić, E. Lidorikis, L. V. Hau, and J. D. Joannopoulos, Phys. Rev. E **71**, 026602 (2005).
[23] W. Yang, A. Joshi, and M. Xiao, Opt. Lett. **29**, 2133 (2004).
[24] H. Wang, D. J. Goorskey, W. H. Burkett, and M. Xiao, Opt. Lett. **25**, 1732 (2000).
[25] C. Sauvan, P. Lalanne, and J.-P. Hugonin, Phys. Rev. B **71**, 165118 (2005).
[26] D. D. Smith, H. Chang, and K. A. Fuller, J. Opt. Soc. Am. B **20**, 1967 (2003).
[27] J. K. Poon, J. Scheuer, and A. Yariv, IEEE Photonics Technol. Lett. **16**, 1331 (2004).
[28] I. Golub, Opt. Lett. **31**, 507 (2006).
[29] L. Y. M. Tobing, D. C. S. Lim, P. Dumon, R. Baets, and M.-K. Chin, Appl. Phys. Lett. **92**, 101122 (2008).
[30] M. F. Yanik and S. Fan, Phys. Rev. Lett. **92**, 083901 (2004).
[31] M. F. Yanik and S. Fan, Phys. Rev. Lett. **93**, 173903 (2004).
[32] Q. Xu, P. Dong, and M. Lipson, Nat. Phys. **3**, 406 (2007).
[33] Q. Xu, J. Shakya, and M. Lipson, Opt. Express **14**, 6463 (2006).
[34] S. Manipatruni, C. B. Poitras, Q. Xu, and M. Lipson, Opt. Lett. **33**, 1644 (2008).
[35] L. Maleki, A. B. Matsko, A. A. Savchenkov, and V. S. Ilchenko, Opt. Lett. **29**, 626 (2004).
[36] D. D. Smith, H. Chang, K. A. Fuller, A. T. Rosenberger, and R. W. Boyd, Phys. Rev. A **69**, 063804 (2004).
[37] A. Naweed, G. Farca, S. I. Shopova, and A. T. Rosenberger, Phys. Rev. A **71**, 043804 (2005).
[38] K. Totsuka, N. Kobayashi, and M. Tomita, Phys. Rev. Lett. **98**, 213904 (2007).
[39] Y. Dumeige, Thi Kim Ngan Nguyên, L. Ghişa, S. Trebaol, and P. Féron, Phys. Rev. A **78**, 013818 (2008).
[40] J. E. Heebner, V. Wong, A. Schweinsberg, R. W. Boyd, and D. J. Jackson, IEEE J. Quantum Electron. **40**, 726 (2004).
[41] H. J. Schmitt and H. Zimmer, IEEE Trans. Microwave Theory Tech. **14**, 206 (1966).
[42] Z. K. Ioannidis, P. M. Radmore, and I. P. Giles, Opt. Lett. **13**, 422 (1988).
[43] J. Morville, D. Romanini, M. Chenevier, and A. Kachanov, Appl. Opt. **41**, 6980 (2002).
[44] J. Poirson, F. Bretenaker, M. Vallet, and A. Le Floch, J. Opt. Soc. Am. B **14**, 2811 (1997).
[45] Y. Dumeige, S. Trebaol, L. Ghişa, T. K. N. Nguyên, H. Tavernier, and P. Féron, J. Opt. Soc. Am. B **25**, 2073 (2008).
[46] H. A. Haus, *Waves and Fields in Optoelectronics* (Prentice-Hall, New York, 1984).
[47] S. Minin, M. R. Fisher, and S. L. Chuang, Appl. Phys. Lett. **84**, 3238 (2004).
[48] J. K. S. Poon, L. Zhu, J. M. Choi, G. A. DeRose, A. Scherer, and A. Yariv, J. Opt. Soc. Am. B **24**, 2389 (2007).